Synthesis of nanostructured materials in supercritical ammonia: Nitrides, metals and oxides

7 **AUTHORS**, INCLUDING:

Cyril Aymonier
French National Centre for Scientific Resea…
137 PUBLICATIONS   **2,101** CITATIONS

SEE PROFILE

Anne Loppinet-Serani
Institut de Chimie de la matière condensée …
43 PUBLICATIONS   **809** CITATIONS

SEE PROFILE

Stephane Gorsse
Institut de Chimie de la matière condensée …
73 PUBLICATIONS   **997** CITATIONS

SEE PROFILE

Synthesis of nanostructured materials in supercritical ammonia: nitrides, metals and oxides

Desmoulins-Krawiec S., Aymonier C., Loppinet-Serani A., Weill F., Grosse S., Etourneau J., Cansell F.

Abstract :

In this study, the synthesis of nanostructured particles of nitrides (Cr_2N, Co_2N, Fe_4N, Cu_3N, Ni_3N), metal (Cu) and oxides (Al_2O_3, TiO_2, Ga_2O_3) by using supercritical ammonia in the reaction medium is described. The elaboration process is based on the thermal decomposition of metal precursors in a supercritical ammonia–methanol mixture at a range of temperatures between 170 and 290 °C at about 16 MPa. Nitrides are obtained at relatively low temperatures in comparison with classical processes. It is shown that the chemical composition of the produced materials can be controlled by the adjustment of process operating conditions (pressure, temperature, metal precursor concentration and residence time in the elaboration reactor) and by the knowledge of the Gibbs free energy of oxide formation of the studied metal.

Introduction :

Today one of the main challenges in materials science concerns the synthesis of nanomaterials since they exhibit interesting properties which can be different of those of bulk materials. For instance, optical, magnetic and electrical properties are sensitive to size effects. Furthermore nanosized particles are equally very efficient in the field of catalysis due to high ratio of surface to volume. Consequently, numerous processes of nanomaterial synthesis have been investigated aiming to control their size, morphology, structure and chemical composition.

In this context, supercritical processes are an interesting alternative to elaborate nanomaterials. A large number of studies concerning the production of nanoparticles have been published. There exist two main routes of material elaboration in supercritical media: processes using a physical transformation (rapid expansion of supercritical solution, gas antisolvent,)[1–4] and less commonly processes using a chemical transformation.[5–8] This work refers to the chemical transformation of metal precursors in a supercritical fluid. More precisely the metal precursor is thermally decomposed to metal atoms which give access to the nucleation and growth of particles.

Previous works devoted to copper particle synthesis in a supercritical mixture CO_2–ethanol demonstrated that this process allows control of the size, the size distribution and the morphology of particles as a function of the operating conditions.[9] In this paper, our objective is to demonstrate the potential of this process to also control the chemical composition of materials.

Many studies have concerned oxide synthesis in supercritical media such as oxide elaboration by hydrothermal synthesis (CeO_2 and $LiCoO_2$)[5,10,11] or the synthesis of $MgAl_2O_4$ in supercritical ethanol.[12] In addition, synthesis of metal particles by supercritical fluid processing has been equally studied: (i) preparation of nickel, cobalt and iron nanoparticles by chemical reduction of $NiCl_2$, $CoCl_2$ and $FeBr_3$, respectively;[13] (ii) copper and silver nanoparticle synthesis in reverse micelles in compressed propane and supercritical ethane solutions;[14,15] (iii) synthesis of silver and copper nanoparticles in a water-in-supercritical carbon dioxide microemulsion by chemical reduction of Ag^+ and Cu^{2+};[16] (iv) the reactive supercritical fluid spray fluid processing method for silver nanoparticles elaboration;[17] (v) radiolytically induced synthesis of silver nanoparticles in supercritical ethane;[18]. Finally, nitride synthesis has been investigated to a lesser extent: (i) the synthesis of TiN in supercritical cryogenic nitrogen by self-propagating-high-temperature synthesis (6.21 MPa, –141 °C);[19] (ii) GaN synthesis by an ammonothermal process (100–500 MPa, 550 °C);[20] (iii) solvothermal synthesis of GaN in supercritical ammonia (100–250 MPa, 400–800 °C);[21] (iv) elaboration of Ni_3N in supercritical ammonia from $Ni(NH_3)_6Cl_2$ ($NaNH_2$, 250 °C and 200 MPa).[22]

In this paper we propose to study the influence of process operating conditions on the control of material nature, and more precisely, on nanostructured nitride elaboration in supercritical ammonia. After a brief description of the experimental set-up and operating conditions, the different types of obtained nanostructured materials as a function of process operating conditions are described.

Experimental :

Experimental set-up

The experimental set-up is a continuous process (Fig. 1). It is composed of two pumps: one for pumping a solvent (NH_3 or CO_2), the other for pumping a cosolvent (methanol or ethanol) to dissolve the metal precursor. The decomposition reaction occurs inside the reactor which is maintained at constant pressure and temperature. The particles elaborated in the reactor are dragged by the flowing fluid to a second vessel (the collector) placed at the outlet of the reactor. In the collector, the particles are stopped by a metal filter placed perpendicularly to the fluid flow. At the end of the experiment, the powder is collected. The powders were dry and free of solvent.

Experiments :

The experimental conditions are summarized in Table 1. Ammonia was chosen as the reaction medium, except for experiment 1, since it exhibits a high reducing power and its critical temperature (T_C = 132.4 °C and P_C = 11.29 MPa) is lower than that of precursor decomposition (most of the metal precursors are thermally decomposed at temperatures above 200 °C). Methanol is used as cosolvent (molar ratio: 70% NH_3–30% methanol) in order to solubilize the metal precursor and to decrease its decomposition temperature (reducing agent).

In the reaction media, there are always traces of oxygen. More precisely, the potential sources of oxygen are: the cosolvent (methanol) and metal precursors (of the acetylacetonate family). The total flow rate was of 1.02 l h^{-1}. Experiment 1 was performed in a supercritical mixture of CO_2–ethanol.

Three types of metal precursors were tested: metal acetylacetonates (acac), metal hexafluoroacetylacetonates (hfac) and a metal diisopropoxide bis(acetylacetonate) $(OPr^i)_2(acac)_2$. All these precursors were provided by Sigma-Aldrich or Strem and used without any further purification. Experimental pressures were about 16 MPa and temperatures between 180 and 290 °C as a function of decomposition temperatures of studied metal precursors.

Characterization

The chemical nature of materials was identified by conventional X-ray powder diffraction (XRPD: Cu-Kα radiation). When crystallized domains were too small to be detected by XRD, electron diffraction was used (JEOL 2000FX microscope); samples were prepared by deposition of a drop of powder dispersed in ethanol on a copper carbon grid. The particle size and morphology were investigated by scanning electron microscopy, SEM (JEOL 840 microscope) and by transmission electron microscopy using the dark field method. The particle size was determined by manual counting.

In a few cases, the materials were amorphous and a thermal treatment was performed from 20 to 1000 °C under argon in a tubular furnace. The thermal treatment led to the crystallization of amorphous materials. The obtained crystalline powder can be characterized by the above methods.

Results and discussion :

Results

The results, structure, chemical composition, morphology and size of crystallized domains of the obtained materials are given in Table 2.

In the case of copper hexafluoroacetylacetonate, the chemical composition of recovered materials depends on the fluid nature. CO_2–ethanol (200 °C–20 MPa) leads to spherical metal copper particles of few micrometers diameter constituted of crystalline nanodomains of about 10 nm (Fig. 2(a)) whilst in NH_3–methanol (200 °C–16 MPa), cubic copper nitride monocrystals (10 µm) were obtained (Fig. 2(b)). The difference of morphology between the metal and nitride has already been discussed[9] and is due to the initial concentration of copper precursor as explained elsewhere.

The synthesis of materials in supercritical NH_3–methanol from nickel and cobalt precursors leads to the pure metal nitrides: nickel nitride and cobalt nitride. As far as Ni_3N and Co_2N particles were concerned, they are organized in shapeless aggregates of a few micrometers constituted of crystalline nanodomains of 20–100 and 60–120 nm, respectively. These materials were identified by XRD and electron diffraction (Fig. 3).

The decomposition of iron and chromium precursors in supercritical NH_3–methanol induces the formation of oxide/nitride mixtures, more precisely, Fe_2O_3/Fe_4N and Cr_2O_3/Cr_2N, as shown in Fig. 4. The mixture Fe_2O_3/Fe_4N is composed of crystalline nanodomains of 10 nm aggregated in spherical particles of 50 nm, so the chemical composition was identified by electron diffraction (Fig. 4). Concerning the second mixture, Cr_2O_3/Cr_2N, it was amorphous after the synthesis thus a thermal treatment was

performed. The obtained material was crystallized and characterized by XRD (Fig. 4(b)). A mixture of Cr_2O_3 and Cr_2N, was synthesized with two different chromium precursors: chromium(III) acetylacetonate and chromium(III) hexafluoroacetylacetonate. Oxides were obtained by decomposition of gallium, titanium and aluminium precursors under the same experimental conditions (supercritical NH_3–methanol). These decompositions were performed at 225–230 °C, 16 MPa (Table 1) and led to the growth of Ga_2O_3, TiO_2 and Al_2O_3, respectively. The Ga_2O_3 and TiO_2 powders are formed by aggregated crystalline nanodomains of 1–10 and 4–50 nm, respectively, as shown in Fig. 5.

In contrast to the above oxides, aluminium oxide was amorphous. The Al_2O_3 particles were spherical particles of about 2 μm (Fig. 6(a)). A thermal treatment was applied to the amorphous material and led to well crystallized aluminium oxide particles as shown in Fig. 6(b).

Discussion :

The choice of the solvent has a great influence on the chemical composition of materials as demonstrated above between syntheses in CO_2 (metallic copper) and NH_3 (copper nitride). CO_2 is an inert solvent whereas NH_3 reacts with the metal atoms to give nitrides. This process of material elaboration in supercritical ammonia allows nitrides to be obtained, in a controlled manner, at relatively low temperature and pressure in comparison with other published methods.[23,24]

Beyond the case of copper, metal nitride formation does not depend only on the solvent choice but also on the nature of the metal. In fact three different behaviours have been observed: nitride formation (Cu_3N, Ni_3N and Co_2N), mixture oxide/nitride formation (Fe_2O_3/Fe_4N and Cr_2O_3/Cr_2N) and oxide formation (Ga_2O_3, TiO_2 and Al_2O_3).

To better understand these results, the affinity of the different studied metals with oxygen was quantified from an Ellingham diagram of oxide formation (Fig. 7). This diagram was obtained from the literature[25] and was completed by the calculation of the curve relative to the formation of Ga_2O_3.[26] This diagram is established at atmospheric pressure but it can be used under our pressure conditions. The pressure dependence of the Gibbs free energy is given by eqn. (1):

$$\Delta G(P) = \Delta G(P_0) + \Delta VP \tag{1}$$

with $\Delta G(P)$, the Gibbs free energy at pressure P, $\Delta G(P_0)$, the Gibbs free energy at pressure P_0 and ΔV, the molar volume.

Furthermore, ΔV is inversely proportional to the Young modulus of the concerned oxide and so can be neglected; in these conditions, we can assume $\Delta G(P) \approx \Delta G(P_0)$.

On the one hand, metals for which the Gibbs free energy of oxide formation is weak (Cu, Ni and Co) tend to only give metal nitrides because the ammonolysis reaction is favoured relative to the metal oxidation reaction by the oxygen atoms dissolved in the reaction media. On the other hand, metals for which the Gibbs free energy of oxide formation is high (Ti and Al) lead to metal oxides.

As far as iron and chromium were concerned, these are located in an intermediate range of affinity with oxygen and there is a competition between ammonolysis and oxidation which involves the formation of mixtures Cr_2O_3/Cr_2N and Fe_2O_3/Fe_4N.

The affinity of gallium with oxygen is in the same range as that of iron and chromium, but only the oxide was obtained. The kinetics of the gallium oxidation reaction seems to be favoured in regard to the thermodynamics.

Conclusions :

Beyond the control of size, size distribution and morphology, the process of material preparation in supercritical media, developed at ICMCB, allows to control the chemical composition of the synthesized nanostructured materials. This process is based on the thermal decomposition of metal precursors in supercritical media, more precisely, in a supercritical ammonia–methanol mixture used in this study.

The thermal decomposition in supercritical ammonia–methanol mixtures of different metal precursors (precursors of Cu, Ni, Co, Fe, Cr, Ga, Al and Ti) was studied at a range of temperatures between 170 and 290 °C at about 16 MPa. Three different mechanisms were observed with the formation of nitrides (Cr_2N, Co_2N, Cu_3N, Ni_3N, Fe_4N), metal (Cu) and oxides (Al_2O_3, TiO_2, Ga_2O_3). In most of the experiments, the synthesized powders were composed of crystalline nanodomains (<100 nm) aggregated in spherical or shapeless particles (except for the Cr

3

and Al compounds which were amorphous).

Thus, the use of supercritical ammonia in the reaction media allows the elaboration of nitrides at relatively low temperatures if the Gibbs free energy of oxide formation of the metal is not too high (Cr, Co, Cu, Ni and Fe). By contrast, only oxides are obtained with metals for which the Gibbs free energy of oxide formation is high (Al and Ti).

Acknowledgements :

References :

1 / Y. Komai, H. Kasai, H. Hirakoso, Y. Hakuta, S. Okada, H. Oikawa, T. Adschiri, H. Inomata, K. Arai and H. Nakanishi, *Mol. Cryst. Liq. Cryst.*, 1998, **322**, 167.

2 / Y. Komai, H. Kasai, H. Hirakoso, Y. Hakuta, H. Katagi, S. Okada, H. Oikawa, T. Adschiri and H. Inomata, *Jpn. J. Appl. Phys.*, 1999, **38**, L81.

3 / E. Reverchon, G. D. Porta, D. Sannino and P. Ciambelli, *Powder Technol.*, 1999, **102**(2), 129 .

4 / J. Jung and M. Perrut, *J. Supercrit. Fluids*, 2001, **20**(3), 179 .

5 / Y. Hakuta, S. Onai, H. Terayama, T. Adschiri and K. Arai, *J. Mater. Sci. Lett.*, 1998, **17**, 1211 .

6 / Y. Hakuta, K. Seino, H. Ura, T. Adschiri, H. Takizawa and K. Arai, *J. Mater. Chem.*, 1999, **9**, 2671 .

7 / T. Adschiri, *Kona (Hirakata Jpn.)*, 1998, **16**, 89.

8 / F. Cansell, B. Chevalier, A. Demourgues, J. Etourneau, C. Even, Y. Garrabos, V. Pessey, S. Petit, A. Tressaud and F. Weill, *J. Mater. Chem.*, 1999, **9**, 67.

9 / V. Pessey, R. Garriga, F. Weill, B. Chevalier, J. Etourneau and F. Cansell, *J. Mater. Chem.*, 2002, **12**(4), 958 .

10 / T. Adschiri, Y. Hakuta and K. Arai, *Ind. Eng. Chem. Res.*, 2000, **39**(12), 4901 .

11 / T. Adschiri, Continuous hydrothermal synthesis of metal oxides in sub- and supercritical water, in *International conference on processing materials for properties*, Minerals, Metals and Materials Society, San Francisco, CA, 2000. 12C. Amiens, D. de Caro, B. Chaudret, J. S. Bradley, R. Mazel and C. Roucau, *J. Am. Chem. Soc.*, 1993, **115**, 11638 .

13 / Y.-P. Sun, H. W. Rollins and R. Guduru, *Chem. Mater.*, 1999, **11**(1), 7.

14J / . P. Cason and C. B. Roberts, *J. Phys. Chem. B*, 2000, **104**(6), 1217.

15 / J. P. Cason, K. Khambaswadkar and C. B. Roberts, *Ind. Eng. Chem. Res.*, 2000, **39**(12), 4749.

16 / H. Ohde, F. Hunt and C. M. Wai, *Chem. Mater.*, 2001, **13**(11), 4130.

17 / H. W. Rollins, *Reactive supercritical fluid preparation of metal and metal-sulfide nanoparticles from carbon dioxide solutions*, in 224th ACS National Meeting, American Chemical Society, Boston, MA, 2000.

18 / N. M. Dimitrijevic, K. Takahashi, D. M. Bartels and C. D. Jonah, *Radiolytically induced synthesis of silver nanoparticles in supercritical ethane*, in 222nd ACS National Meeting, American Chemical Society, Chicago, 2001.

19 / K. Brezinsky, J. A. Brehm, C. K. Law and I. Glassman, *Supercritical combustion synthesis of titanium nitride*, in *Twenty-sixth symposium (International) on combustion*, Napoli, Italy, July 28–August 2, ed. A. R. Burgers, The Combustion Institute, Pittsburgh, 1996, vol. 2, p. 1875.

20 / R. Dwilinski, A. Wysmolek, J. Baranowski, M. Kaminska, R. Doradzinski, J. Garczinski, L. Sierzputowski and H. Jacobs, *Acta. Phys. Pol. A*, 1995, **88**(5), 833.

21 / C. Collado, G. Demazeau, B. Berdeu, A. Largeteau, J.-C. Garcia, J.-L. Guyaux and J. Massies, in *Chimie de l'état solide et cristallochimie/Solid state chemistry and crystallochemistry*, C. R. Acad. Sci., Ser. 2c: chim., Paris, 1999, p. 483.

22 / A. Leineweber, H. Jacobs and S. Hull, *Inorg. Chem.*, 2001, **40**, 5818.

23 / F. Attar and T. Johannesson, *Thin Solid Films*, 1995, **258**, 205.

24 / N. S. Gajbhiye, R. S. Ningthoujam and J. Weissmüller, *Phys. Status Solidi A*, 2002, **189**(3), 691.

25 / J. Philibert, A. Vignes, Y. Bréchet and P. Combrade, *Métallurgie du minerai au matériau*, Masson, Paris, 1998.

26 / M. Stan, T. J. Armstrong, D. P. Butt, T. C. Wallace, Sr., Y. S. Park, C. L. Haertling, T. Hartmann and R. J. Hanrahan, Jr., *J. Am. Ceram. Soc.*, 2002, **85**(11), 2811.

Table 1 Experimental conditions

Test	Precursor	Fluid	Precursor concentration in cosolvent (g/g)	$T/°C$
1	$Cu(hfac)_2$	CO_2	4.1×10^{-2}	200
2	$Cu(hfac)_2$	NH_3	4×10^{-3}	200
3	$Ni(hfac)_2$	NH_3	4×10^{-3}	290
4	$Co(hfac)_2$	NH_3	4×10^{-3}	260
5	$Fe(acac)_3$	NH_3	4×10^{-3}	180
6	$Cr(hfac)_3$	NH_3	2×10^{-3}	260
7	$Cr(acac)_3$	NH_3	4×10^{-3}	230
8	$Ga(acac)_3$	NH_3	1.7×10^{-3}	225
9	$Al(acac)_3$	NH_3	4×10^{-3}	225
10	$Ti(OPr^i)_2(acac)_2$	NH_3	6×10^{-3}	230

Table 2 Chemical composition, structure, morphology and size of crystallized domains of synthesized nanostructured materials

| Test	Chemical composition	Structure	Morphology	Size of crystallized domains
1	Cu	Cubic, a = 3.6150 Å	Spherical aggregates	10 nm
2	Cu_3N	Cubic, a = 3.8171 Å	Cubic monocrystals	10 µm
3	Ni_3N	Hexagonal, a = 4.6224 Å, c = 4.3059 Å	Shapeless aggregates	20–100 nm
4	Co_2N	Orthorhombic, a = 2.8535 Å, b = 4.6056 Å, c = 4.3443 Å	Shapeless aggregates	60–120 nm
5	Fe_2O_3 + Fe_4N	Cubic, a = 8.3515 Å; cubic, a = 3.7950 Å	Shapeless aggregates	5–60 nm
6	Cr_2O_3 + Cr_2N	Amorphous	Shapeless aggregates	—
7	Cr_2O_3 + Cr_2N	Amorphous	Shapeless aggregates	—
8	Ga_2O_3	Monoclinic, a = 12.2271 Å, b = 3.0389 Å, c = 5.8079 Å, β = 103.82°	Shapeless aggregates	1–10 nm
9	TiO_2	Tetragonal (rutile), a = 4.5933 Å, c = 2.9592 Å	Shapeless aggregates	4–50 nm
10	Al_2O_3	Amorphous	Spherical particles	—
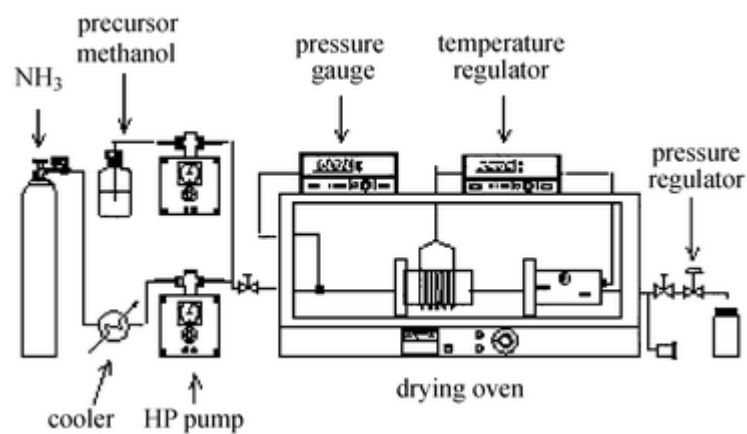
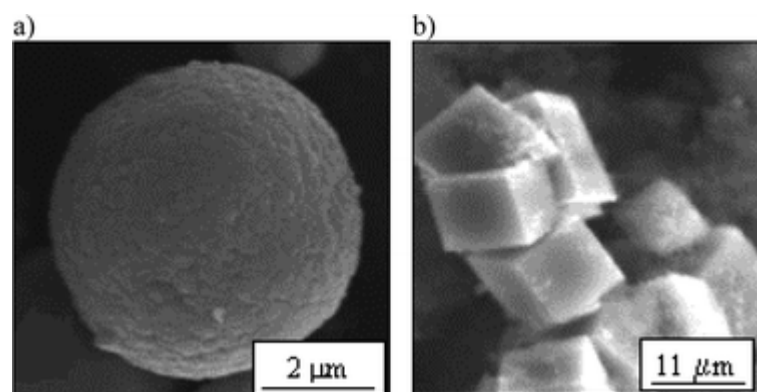**Fig. 1** Experimental set-up for material synthesis in supercritical fluid.

Fig. 2 Influence of reaction media on the particle chemical composition: (a) SEM image of a spherical nanostructured copper particle, (b) SEM image of cubic copper nitride monocrystals.
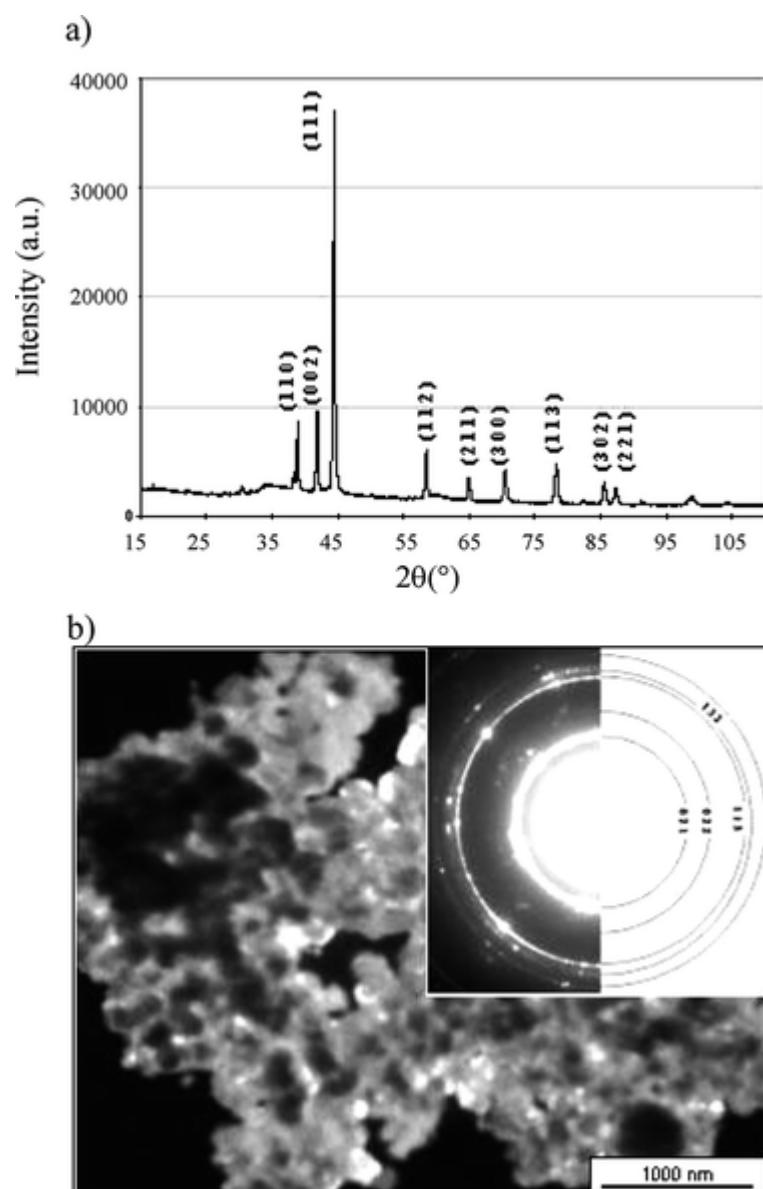
Fig. 3 (a) XRD pattern of Ni$_3$N and (b) microscopic and electronic characterization of Co$_2$N.
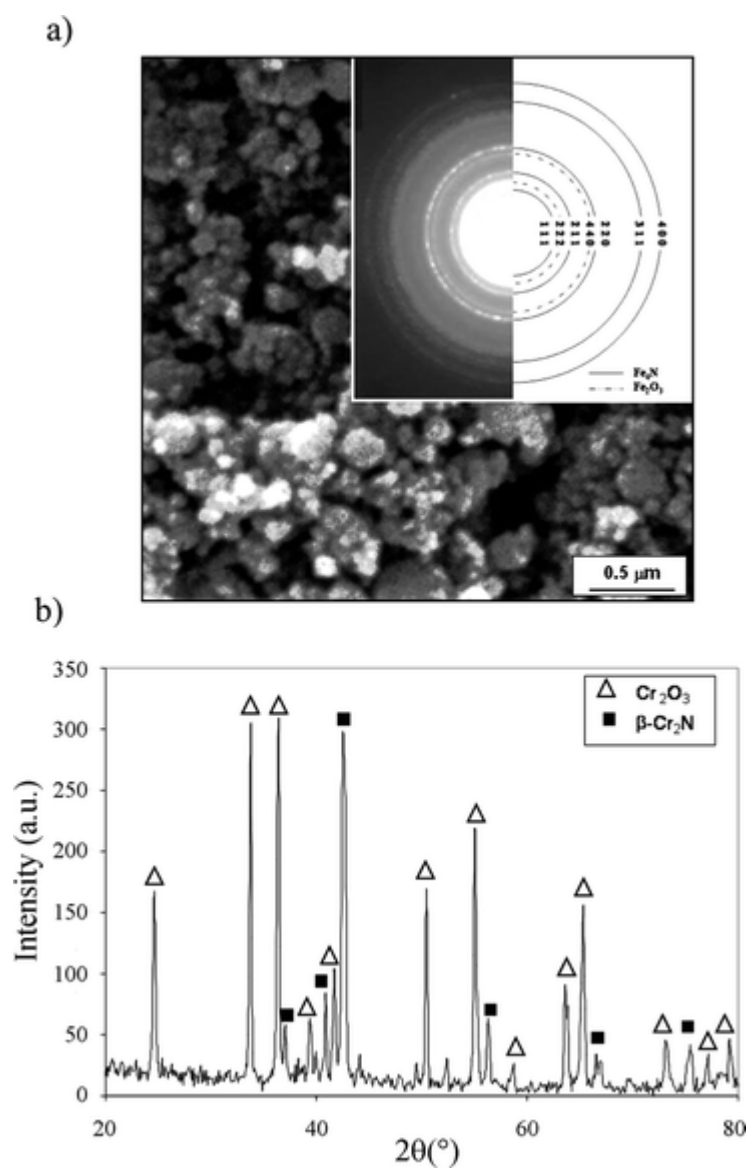
8

Fig. 4 Structural characterization of mixtures Fe_2O_3/Fe_4N and Cr_2O_3/Cr_2N: (a) electron diffraction pattern and SEM image of Fe_2O_3/Fe_4N, (b) XRD pattern of Cr_2O_3/Cr_2N.
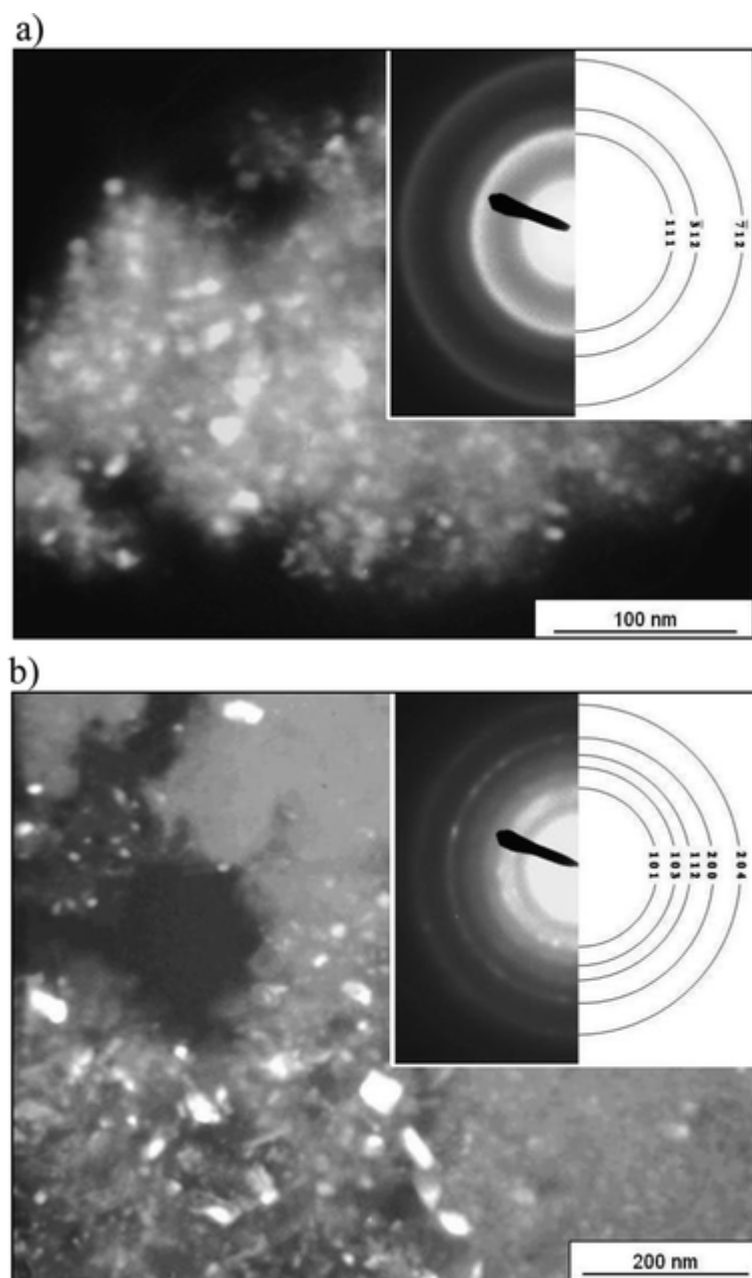
Fig. 5 TEM images and electron diffraction patterns of (a) Ga_2O_3 and (b) TiO_2.
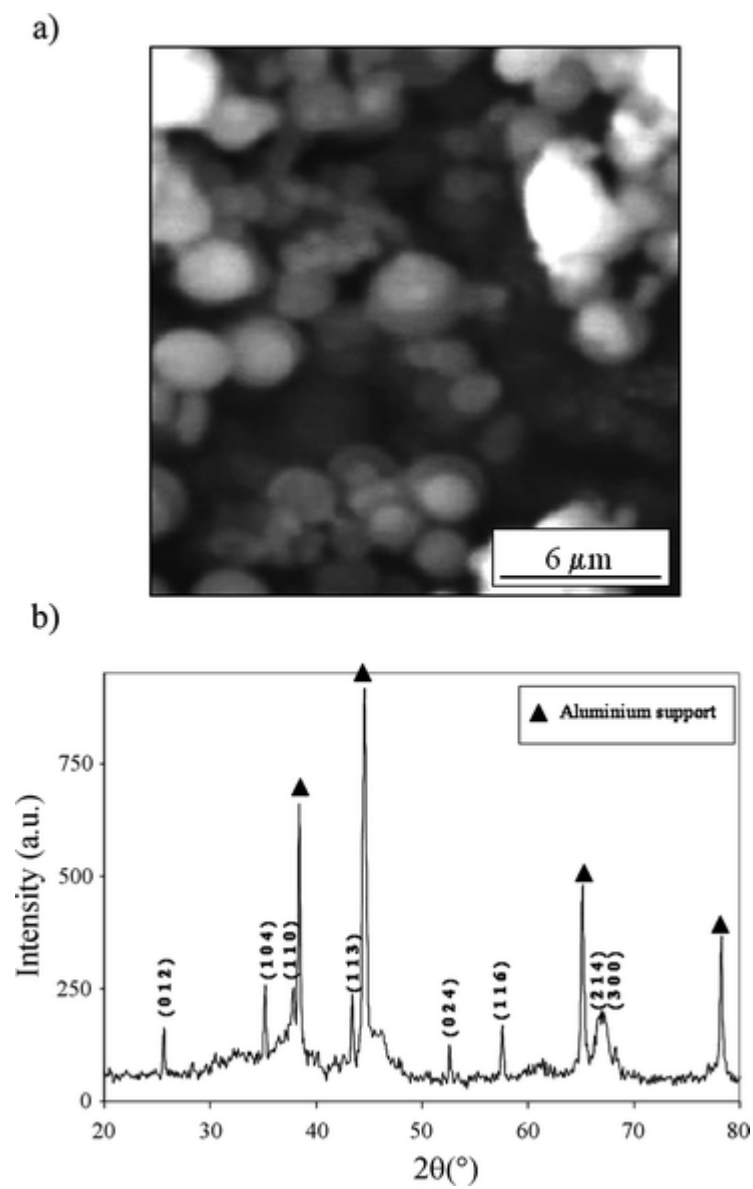
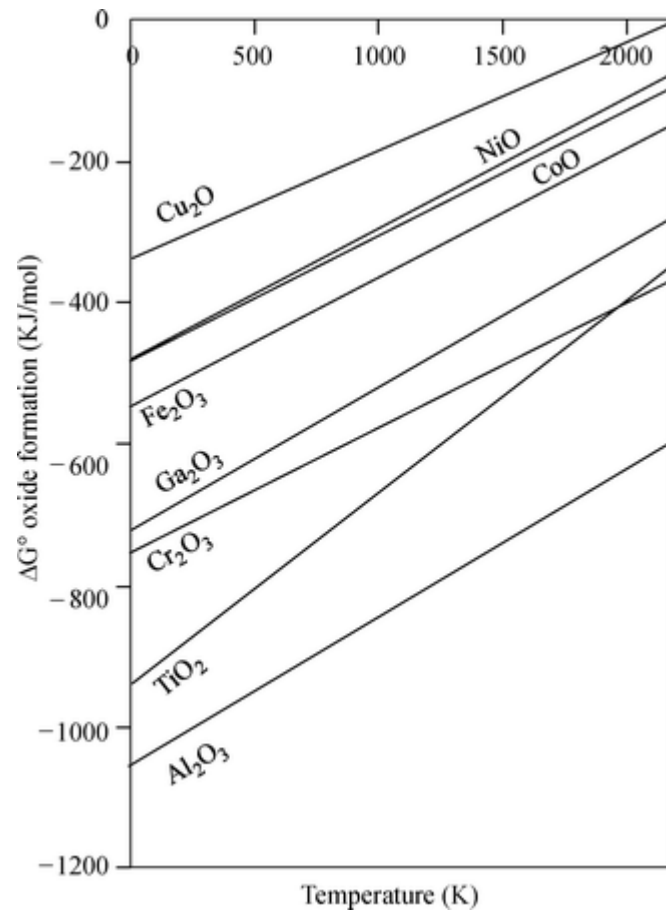**Fig. 6** SEM image of amorphous Al_2O_3(after synthesis) and XRD pattern of crystallized Al_2O_3(after thermal treatment).

11

Fig. 7 Ellingham diagram of oxide formation.

12